Tailoring light emission properties of fluorophores by coupling to resonance-tuned metallic nanostructures

Sebastian Gerber, Frank Reil, Ulrich Hohenester, Thomas Schlagenhaufen, Joachim R. Krenn, and Alfred Leitner*
Institut für Physik, Karl-Franzens-Universität Graz, Universitätsplatz 5, 8010 Graz, Austria
(Received 15 December 2006; published 6 February 2007)

We report the enhancement of the radiative decay rate of Eu^{3+} fluorophores by coupling them to nanoscopic gold disks located on a substrate. When the plasmon resonance frequency of the disks coincides with the fluorophore emission frequency, each disk acts as a supplemental antenna for the fluorophore by converting its nonradiative near field into radiating far field, thereby increasing its radiative decay rate dramatically. The radiative rate is measured by time-correlated single-photon counting for resonant and nonresonant metallic nanodisks. Supplementary theoretical model calculations are found to be in remarkably good agreement with the experiment.

DOI: 10.1103/PhysRevB.75.073404 PACS number(s): 78.67.Bf, 33.50.−j, 42.50.Ct, 78.47.+p

Nanometer-sized metal particles support localized surface plasmons associated with the collective oscillations of conduction-band electrons.[1] These modes are characterized by spectrally selective absorption and scattering, and can give rise to a drastic enhancement of local electromagnetic fields. As a consequence, the fluorescence and Raman properties of molecules located in the proximity of metallic nanoparticles become strongly modified, which can be exploited for a variety of applications, such as surface-enhanced Raman scattering[2,3] or biochemical sensorics.[4] Improved nanofabrication methods nowadays allow advanced control of the nanoparticle shape and the arrangement of nanoparticle ensembles,[5] and open the possibility to flexibly tailor specific molecule-nanoparticle couplings. However, hitherto the detailed understanding of this coupling has been hindered by the intricate interplay of excitation enhancement, and radiative and nonradiative decay processes, which all strongly depend on the local optical environment in which the molecule is embedded. To overcome this deficiency, Anger *et al.*[6] recently investigated the fluorescence of a single molecule close to a single spherical gold nanoparticle, and demonstrated, by varying the molecule-nanoparticle distance, the continous transition from fluorescence enhancement to fluorescence quenching.[7] This finding was supported by Kühn and co-workers[8] using a similar setup, but with the particle plasmon resonance tuned to the molecular excitation frequency. In both of these experiments an increase in the total fluorescence has been measured. This increase was attributed to both excitation- and de-excitation rate enhancements with the help of numerical analysis of the experimentally determined parameters.

In this paper, we introduce a complementary scheme which enables the direct measurement of the radiative de-excitation enhancement without the need for additional data processing. We employ nanofabricated disk-shaped gold particles with the plasmon resonance exactly fitting the fluorescence-as opposed to the excitation frequency, and a fluorophore with an extremely large Stoke shift. Here, the molecule is excited at a frequency far beyond the nanoparticle plasmon resonance. In contrast to previous works this gives us the unique possibility to manipulate the de-excitation process without affecting the excitation rate, which is practically not influenced by the presence of the metallic particle. On the other side, the decay process becomes strongly altered by the nanoparticle, which acts as a supplemental antenna and converts part of the fluorophore's near field into radiation. This can be directly observed in our time-resolved fluorescence decay measurements as an enhancement of the initial fluorescence intensity. Because of the comparatively low radiative decay rate of the fluorophore class our dye belongs to, we use an ensemble of molecules which are positioned at random distances to the metal discs. In the collective fluorescence decay, subsequent to the excitation by a sufficiently short pulse, the molecules at different positions contribute differently to the radiation, thus leading to a strongly nonexponential decay. The stronger the radiative rate enhancement, the more the molecules contribute at the beginning of the decay, which allows us to discriminate between molecules close to and far away from the nanoparticle, and which might be beneficial for labelling purposes in future biosensors. Our experimental study is supplemented by a theoretical analysis based on the boundary-element method,[9] whose results are in remarkably good agreement with experimental data. From this comparison we infer an up to hundredfold enhancement of the radiative decay rate for short molecule-nanoparticle distances.

Consider a single excited fluorescent molecule located at a few nanometers from the nanoparticle. The oscillating near field of the decaying molecule generates a localized surface plasmon polariton in the particle, when their respective frequencies are close. Most efficiently in the resonant case, energy is transferred from the molecule to the particle and radiated off. This additional radiative decay channel increases the radiative rate γ_r. In addition, Ohmic losses of the plasmon oscillations and other dissipative effects lead to a larger nonradiative decay rate γ_{nr}.[6] The radiative yield $q_a = \gamma_r/\gamma$ is the probability that the excited molecule decays by emitting a photon, with $\gamma = \gamma_r + \gamma_{\mathrm{nr}}$ being the total decay rate. In a continuous-wave experiment the fluorescence intensity is proportional to $q_a \gamma_{\mathrm{exc}}$, where γ_{exc} is the molecular excitation rate, and the respective importance of γ_r and γ_{nr} to the radiative yield can only be exctracted by support of a supplementary theoretical analysis. Things are more favorable for time-resolved measurements. Suppose that the molecule is

initially excited by a short laser pulse, and the subsequent internal molecular relaxation is much faster than the radiative and nonradiative decay times, which is generally the case. Then, the time evolution of the fluorescence intensity is proportional to $\gamma_r e^{-\gamma t}$, and the initial fluorescence intensity is a direct measure of γ_r whereas the decay constant directly yields the total decay rate γ. It is important to realize that these conclusions also hold for molecular ensembles, where the fluorescence decay subsequent to a fast excitation is according to

$$I(t) \propto \langle \gamma_r e^{-\gamma t} \rangle, \tag{1}$$

the bracket denoting an appropriate average over molecule positions. In Eq. (1) the intensity $I(t=0)$ determines the average enhancement of γ_r, and the shape of the fluorescence decay provides direct information about the distribution of the decay rates γ.

In our experiment, we perform time-resolved single-photon counting measurements on europium(III)-thenoyltrifluoroacetonate fluorophores (EuTTA) randomly distributed on a two-dimensional array of gold nanodisks. For the excitation of the fluorophore we use pulsed UV laser diode light at $\lambda = 375$ nm, with an effective pulse width of 10 μs and a repetition rate of 365 Hz, in a conventional commercial fluorescence microscope with a 50×, numerical aperture (NA)=0.85 objective. A time-correlated single-photon-counting setup repeatedly measures the time interval between the excitation laser pulse and the detected fluorescence photons and stores the corresponding values in a multichannel analyzer with a bin width of 1 μs, which is read out after typically a few thousand sweeps.

We have fabricated two kinds of samples, each consisting of a quadratic array of gold nanodisks on a silicon dioxid substrate, which were produced by electron-beam lithography. Figure 1(a) shows their size parameters and mutual distances as well as their electron-microscopic images. Their absorbance spectra are compared with the emission line of our EuTTA fluorophore in Fig. 1(b). The resonant disks match the EuTTA emission wavelength of 612 nm, the non-resonant disks are approximately 50 nm off. The large distance $\geqslant$50 nm between the disks ensures that coupling effects can be neglected, which was also confirmed by numerical simulations. The EuTTA deposition was carried out by vacuum sublimation, resulting in a homogeneous film corresponding to a coverage of about ten monolayers.

Figure 2(a) shows the measured fluorescence curves (dots) and their fits (solid lines) for the disks in and off resonance with the molecule emission as well as for the fluorophore on the bare substrate. We shall find it convenient to fit the data by a stretched exponential[10,11]

$$I(t) \propto \exp[-(\gamma_p t)^{\beta}], \tag{2}$$

with γ_p a pseudodecay rate and β a constant that determines the distribution of decay rates. The shape (2) provides excellent agreement with the experimental data throughout, and has the advantage that it allows us to directly obtain a decay rate distribution, as will be discussed further below. The solid line in Fig. 2(b) shows the fluorescence decay for a molecule ensemble on the silicon dioxide surface without

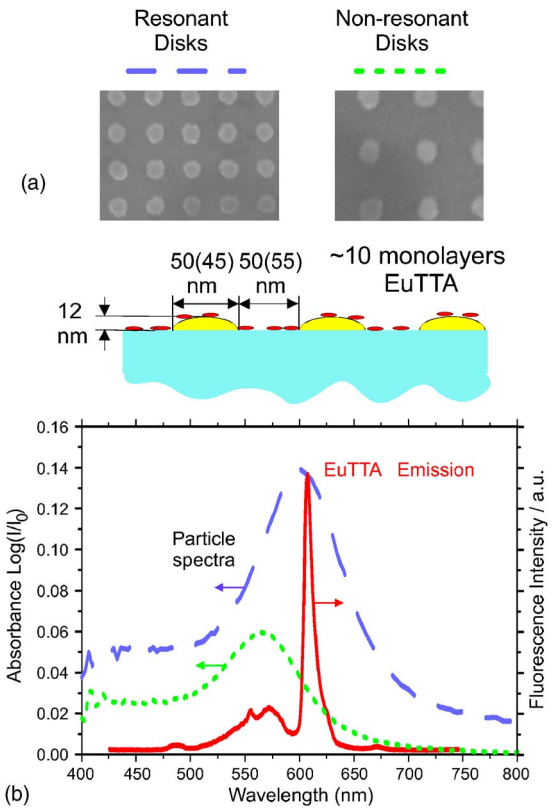

FIG. 1. (Color online) (a) Electron-microscopic image and sample makeup of our resonant and off-resonant gold disk samples. All size parameters: ±3 nm. (b) Emission spectrum of EuTTA fluorophore (solid line), absorbance spectra of resonant (dashed line), and off-resonant disks (dotted line). All wavelengths: ±3 nm.

gold particles. Its decay is almost monoexponential, with only small deviations associated to slight differences in the dielectric nanoenvironment and unspecified quenchers. It has been pointed out though that there is no orientational convolution in the fluorescence curve which could explain the contributions of other decay rates, since the europium atom rotates in its chelate enclosure at a much higher frequency than the decay rates involved. The molecule's projected local density of states (LDOS), which determines its decay rate, is therefore proportional to its orientation-averaged LDOS.[12] The fluorescence decay changes dramatically in the presence of metallic nanoparticles. The initial fluorescence intensity is enhanced by a factor of 5 for the resonant particles and a factor of 2.5 for the off-resonant ones, thus indicating, according to Eq. (1), an overall enhancement of γ_r by the same factors. The subsequent decay is shortened by almost two orders of magnitude. This clearly shows that the genuine emission properties of excited molecules are drastically modified in the presence of near-field coupling to metallic nanoparticles. For comparison, in Fig. 2(b) we plot the strongly quenched fluorescence of molecules on a flat gold surface.

The area below the luminescence curve is proportional to the radiative yield q_a of the fluorescing system. The A values in Fig. 2(b) denote the measured area of the respective curves in arbitrary units. Except for the almost entirely quenched fluorophores on the flat gold film, the resonant

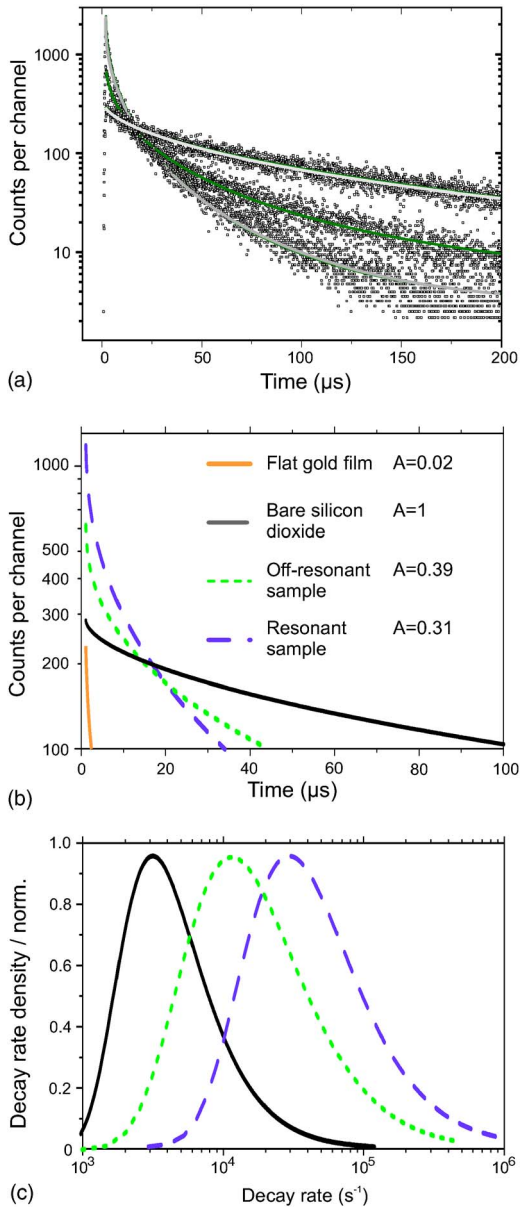

FIG. 2. (Color online) (a) Raw fluorescence data (dots) and fits [solid lines, see (b)]. (b) Fitted fluorescence curves of gold on flat metal film (yellow line in lower left corner), on bare silicon dioxide substrate (black solid line) and on resonant and off-resonant samples (dashed and dotted lines). (c) Decay rate density distributions corresponding to fluorescence curves in (b).

sample system shows the smallest q_a, followed by the nonresonant sample. This indicates that, together with the enhancement of the radiative decay rate, the nonradiative decay rate is strongly increased too, which can be traced back to Ohmic power loss inside the nanodisks. We can use the stretched exponential form (2) to extract a distribution of total decay rates according to the prescription of Refs. 10 and 11. Figure 2(c) shows the calculated decay rate density for each curve (except for the flat gold film). The average decay rate and the corresponding width increase considerably from the fluorophore on the silicon dioxide surface over the off-resonance to the on-resonance sample.

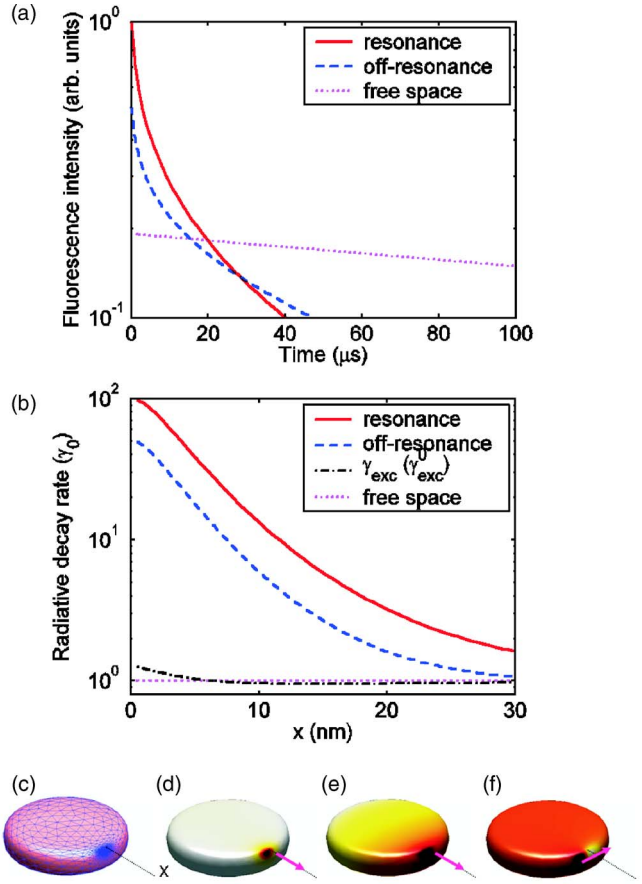

FIG. 3. (Color online) Results of our theoretical BEM calculations for a particle with 50 nm diameter and 12 nm height. (a) Temporal fluorescence decay of molecule ensemble situated in a ring of 30 nm width around the gold nanoparticle, and for molecule transition frequencies of plasmon resonance (610 nm, solid line) and off-resonance (590 nm, dashed line). The dotted line shows the fluorescence of the same ensemble in absence of the nanoparticle. (b) Radiative decay rate as a function of particle-molecule distance in units of the free radiative decay rate γ_0. The dashed-dotted line reports the excitation enhancement[6] at the exciting wavelength of 375 nm. (c) Triangulated surface of disk-shaped particle used in our calculations. Density plot of (d) real and (e) imaginary part of surface charge induced by dipole located at a distance of 5 nm away from the nanoparticle and with dipole orientated along x. (f) Same as (e) but for dipole orientation along y.

To confirm our conclusions we additionally performed theoretical model calculations. Following Refs. 6 and 8 we adopt the quasistatic approximation and include retardation effects by means of an effective polarizibility.[13] For the calculation of γ_r, γ_{nr}, and γ_{exc} we employ the boundary element method (BEM).[9,14] Consider a molecule with dipole moment $\boldsymbol{d}$ located at position $\boldsymbol{r}_m$ in the vicinity of the metallic nanoparticle. The electric field $\boldsymbol{E}_{dip}$ produced by the dipole will exert a force on the charge distribution of the nanoparticle. Within the BEM approach the response of the metallic particle is described by means of a surface charge $\sigma(\boldsymbol{s})$, which is determined such that the boundary conditions of Maxwell's theory are fulfilled at the boundary of the metallic nanoparticle.[14] We approximate the particle surface by a set

of triangles, see Fig. 3(c) and consider within each triangle σ as constant. Typically a few thousand triangles are used, whose sizes decrease with decreasing distance to the molecule in order to resolve the strong variations of σ in the vicinity of $\boldsymbol{r}_m$. For the dielectric function of the gold particle we use the tabulated values of Johnson and Christie,[15] and assume that the particles are embedded in a medium of dielectric constant $\epsilon_b=2.25$. Within this approach we can compute the enhancement of the radiative decay rate from the total dipole moment of the molecule and the induced surface charge σ, whereas the nonradiative decay rate due to Ohmic losses is proportional to the imaginary part of $\boldsymbol{d}\cdot\boldsymbol{E}(\boldsymbol{r}_m)$.[6] Finally, to compute the excitation enhancement γ_{exc} we simply replace in our BEM approach the electric field $\boldsymbol{E}_{\mathrm{dip}}$ of the dipole by the constant field $\boldsymbol{E}_0$ of the exciting laser.

Figure 3(b) shows the enhancement of the radiative decay rate as a function of molecule-particle separation and for a disk-shaped nanoparticle with 50 nm diameter and 12 nm height. These parameters were chosen such that the plasmon resonance matches the experimental value of approximately 610 nm. For the off-resonant excitation we keep for simplicity the particle shape fixed and only set the dipole excitation frequency to 590 nm. We assume that the molecular dipole is oriented either along x, Figs. 3(d) and 3(e), or y, Fig. 3(f), and average over these two different orientations. Our results reveal that for small distances γ_r becomes boosted by a factor of 100 and 50 for the resonant and nonresonant case, respectively. In addition we observe a drastic enhancement of γ_{nr} (not shown), which is approximately by a factor of 10 larger than γ_r over a wide range of distances, such that the radiative yield becomes substantially reduced. A closer inspection of the surface charge distributions shown in Figs. 3(d)–3(f) shows that the real part of σ is reminiscent of the distribution produced by a mirror dipole inside the particle, whereas the imaginary part is reminiscent of the dipole mode of plasmonic oscillations[9] responsible for the enhancement of γ_r. In the figure we also observe that the excitation enhancement $\gamma_{\mathrm{exc}}/\gamma_{\mathrm{exc}}^0$ at the exciting wavelength of 375 nm is close to unity for all distances, in accordance to our previous assumption, that we can neglect any excitation rate modifications. In the following we set for simplicity $\gamma_{\mathrm{exc}}=\gamma_{\mathrm{exc}}^0$. To compare our results with the experimental fluorescence decay data we proceed as follows. We consider a single nanoparticle and assume that the molecules are located in a ring of 30 nm width around the particle, corresponding to the effective active area of one nanoparticle in the square arrangement of the experiments. The fluorescence intensity is then obtained by averaging over the molecule positions x and dipole orientations θ according to

$$I(t) \propto \int_{25\ \mathrm{nm}}^{50\ \mathrm{nm}} x dx \int_0^{2\pi} d\theta \gamma_r(x,\theta) e^{-\gamma(x,\theta)t}. \tag{3}$$

The total decay rate is the sum of γ_r, Ohmic losses, and molecular nonradiative decay channels γ_m that is related to the free radiative decay rate γ_0 through the quantum yield $q_m=\gamma_0/(\gamma_0+\gamma_m)$. We use $q_m=\frac{1}{3}$ and $q_m/\gamma_0=400$ μs. Figure 3 shows the fluorescence decay for a molecule ensemble as computed within this approach. The results compare nicely with the experimental data shown in Fig. 2. Again, the initial fluorescence and the fluorescence decay constant are strongly enhanced in presence of metallic nanoparticles.

We have experimentally and theoretically demonstrated the substantial increase of the radiative decay rate of EuTTA fluorophores by coupling to specially tailored metallic nanoparticles. In our experiment, we can entirely neglect any modifications of the fluorophore excitation rate. This enables us to selectively investigate the de-excitation processes, without the need for introducing numerical data processing to suppress difficult-to-quantify contributions from the excitation process. In future experiments, we plan to optimize shape and arrangement of the metallic nanoparticles in the search for even stronger radiative decay rate enhancements. Such nanoarray devices could be the basis for a new generation of biochemical sensor principles.

*Electronic address: alfred.leitner@uni-graz.at; http://nanooptics.uni-graz.at

[1] U. Kreibig and M. Vollmer, *Optical Properties of Metal Clusters*, Springer Series in Material Science Vol. 25 (Springer, Berlin, 1995).
[2] M. Moskovits, Rev. Mod. Phys. **57**, 783 (1985).
[3] H. Xu, X.-H. Wang, M. P. Persson, H. Q. Xu, M. Kall, and P. Johansson, Phys. Rev. Lett. **93**, 243002 (2004).
[4] A. Haes and R. P. V. Duyne, J. Am. Chem. Soc. **124**, 10596 (2002).
[5] W. Rechberger, A. Leitner, A. Hohenau, J. R. Krenn, and F. R. Aussenegg, Opt. Commun. **220**, 137 (2003).
[6] P. Anger, P. Bharadwaj, and L. Novotny, Phys. Rev. Lett. **96**, 113002 (2006).
[7] E. Dulkeith, M. Ringler, T. A. Klar, J. Feldmann, A. Munoz Javier, and W. J. Parak, Nano Lett. **5**, 585 (2005).
[8] S. Kühn, U. Håkanson, L. Rogobete, and V. Sandoghdar Phys. Rev. Lett. **97**, 017402 (2006).
[9] U. Hohenester and J. Krenn, Phys. Rev. B **72**, 195429 (2005).
[10] H. Pollard, Bull. Am. Math. Soc. **52**, 908 (1946).
[11] C. P. Lindsey and G. D. Patterson, J. Chem. Phys. **73**, 3348 (1980).
[12] W. L. Barnes, J. Mod. Opt. **45**, 661 (1998).
[13] T. Kalkbrenner, U. Håkanson, and V. Sandoghdar, Nano Lett. **4**, 2309 (2004).
[14] F. J. Garcia de Abajo and A. Howie, Phys. Rev. B **65**, 115418 (2002).
[15] P. B. Johnson and R. W. Christy, Phys. Rev. B **6**, 4370 (1972).